

Supporting Information

Fenton-Reaction-Accelerable Magnetic Nanoparticles for Ferroptosis Therapy of Orthotopic Brain Tumors

Zheyu Shen,^{†,‡} Ting Liu,[§] Yan Li,^Δ Joseph Lau,[‡] Zhen Yang,[‡] Wenpei Fan,[‡] Zijian Zhou,[‡] Changrong Shi,[§] Chaomin Ke,[§] Vladimir I. Bregadze,[‡] Swadhin K. Mandal,[°] Yijing Liu^{*,‡}, Zihou Li,[†] Ting Xue,[†] Guizhi Zhu,[‡] Jeeva Munasinghe,[#] Gang Niu,[‡] Aiguo Wu,^{*,†} Xiaoyuan Chen^{*,‡}

[†] CAS Key Laboratory of Magnetic Materials and Devices, & Key Laboratory of Additive Manufacturing Materials of Zhejiang Province, & Division of Functional Materials and Nanodevices, Ningbo Institute of Materials Technology and Engineering, Chinese Academy of Sciences, 1219 Zhong-guan West Road, Ning-bo, Zhe-jiang 315201, China.

[‡] Laboratory of Molecular Imaging and Nanomedicine, National Institute of Biomedical Imaging and Bioengineering, National Institutes of Health, Bethesda, Maryland 20892, United States.

[§] State Key Laboratory of Molecular Vaccinology and Molecular Diagnostics & Center for Molecular Imaging and Translational Medicine, School of Public Health, Xiamen University, Xiamen, 361102, China.

^Δ Key Laboratory of Applied Marine Biotechnology of Ministry of Education, Ningbo University, Ningbo 315211, China.

[‡] A.N. Nesmeyanov Institute of Organoelement Compounds of Russian Academy of Sciences, Vavilov Str. 28, Moscow 119991, Russia.

[°] Department of Chemical Sciences, Indian Institute of Science Education and Research-Kolkata, Mohanpur-741246, India.

[#] Mouse Imaging Facility, National Institute of Neurological Disorder and Stroke, National Institutes of Health, Bethesda, Maryland 20892, United States.

Corresponding Authors

*E-mail: shawn.chen@nih.gov

*E-mail: aiguo@nimte.ac.cn

*E-mail: yijing.liu@nih.gov

Materials and Methods

Materials. Poly(acrylic acid) (PAA, Mw = 1800), iron (III) chloride (FeCl_3 , $\geq 97\%$), gadolinium (III) nitrate hexahydrate ($\text{Gd}(\text{NO}_3)_3 \cdot 6\text{H}_2\text{O}$, 99.9%), *N*-(3-Dimethylaminopropyl)-*N'*-ethylcarbodiimide (EDC, $\geq 97\%$), *N*-hydroxysuccinimide (NHS, 98 %), cisplatin (CDDP), lactoferrin (LF), Rhodamine 6G (R6G), phalloidin-FITC, and Hoechst 33258, 2,7-dichlorofluorescein diacetate (DCF-DA), deferoxamine mesylate (DFO) and *N*-Acetyl-L-cysteine (NAC) were purchased from Sigma-aldrich (USA). Iron (II) sulfate heptahydrate ($\text{FeSO}_4 \cdot 7\text{H}_2\text{O}$) was purchased from Acros organics. Glu-{Cyclo[Arg-Gly-Asp-(D-Phe)-Lys]}₂ (*i.e.* RGD dimer, or RGD2, 97.92%, Mw = 1318.51) was purchased from C S Bio Co. (CA, USA 94025).

Release behaviors of Fe and Pt from FeGd-HN@Pt2@LF/RGD2. The release behavior of Fe and Pt from FeGd-HN@Pt2@LF/RGD2 was determined by ICP-OES at pH 5.5 or 7.4. Typically, 3.0 mL of FeGd-HN@Pt2@LF/RGD2 ($C_{\text{Fe}}=2.80$ mM, $C_{\text{Gd}}=1.37$ mM, $C_{\text{Pt}}=0.34$ mM) was respectively added in 10 mL of PBS with pH value of 5.5 or 7.4. The solutions with various pH values were kept in a shaking incubator (Excella E24, New Brunswick Scientific) at 37 °C. At predetermined time intervals, 1.0 mL of the solutions with different pH values were taken and subjected to centrifugal ultrafiltration (Millipore, molecular size cutoff of 30 kDa). The supernatants were then determined by ICP-OES. The Fe or Pt release behavior at different pH values was monitored *via* plot of the cumulative released Fe or Pt content (*i.e.* the molar percentage of the released Fe or Pt to the total amount of Fe or Pt in FeGd-HN@Pt2@LF/RGD2) as a function of incubation time.

Cell culture. U-87 MG (human glioblastoma cell line), and cisplatin-resistant MCF-7 (Human breast cancer cell line) cells were cultured in the DMEM medium supplemented with 10 wt% of fetal bovine serum (FBS), 100 units/mL of penicillin and 100 $\mu\text{g}/\text{mL}$ of streptomycin. HBEC-5i (human brain microvascular endothelial cell line) cells were cultured in the DMEM:F12 medium supplemented with 40 $\mu\text{g}/\text{mL}$ endothelial growth supplement, 10 wt % of FBS, 100 units/mL of penicillin and 100 $\mu\text{g}/\text{mL}$

of streptomycin. The cells were incubated at 37 °C in a humidified atmosphere containing 5 % of CO₂.

Synthesis of Rhodamine 6G-Loaded FeGd-HN@Pt2 or FeGd-HN@Pt2@LF/RGD2. To investigate the internalization of FeGd-HN@Pt2 or FeGd-HN@Pt2@LF/RGD2 in cells by flow cytometry and laser scanning confocal microscopy (LSCM), Rhodamine 6G (R6G) was loaded onto the surface of FeGd-HN@Pt2 or FeGd-HN@Pt2@LF/RGD2. Typically, 4.0 mL of FeGd-HN@Pt2, or FeGd-HN@Pt2@LF/RGD2 ($C_{Fe}=2.80$ mM) were mixed with 0.7 mL of Rhodamine 6G (10 μM) under magnetic stirring at room temperature. After 24 h, the obtained R6G@FeGd-HN@Pt2 or R6G@FeGd-HN@Pt2@LF/RGD2 solution was washed using Milli-Q water by centrifugal ultrafiltration (Millipore, molecular size cutoff of 10 kDa) to remove unloaded R6G. The finally obtained R6G@FeGd-HN@Pt2 or R6G@FeGd-HN@Pt2@LF/RGD2 was dispersed in 4.0 mL of Milli-Q water.

Cellular uptake by laser scanning confocal microscopy (LSCM). Uptake of the nanoparticles by U-87 MG, or MCF-7 cells was studied using LSCM. Typically, 0.5 mL of U-87 MG, or MCF-7 cells in growth medium were seeded into each well of Falcon® Culture Slide (8 Well, Corning) at a density of 1.0×10^5 cells/mL and allowed to adhere at 37 °C for 24 h. The growth medium was replaced with a fresh one (0.5 mL, without FBS) containing R6G@FeGd-HN@Pt2 or R6G@FeGd-HN@Pt2@LF/RGD2 ($C_{Fe} = 10$ μM). After further 2 h incubation, the cells were washed twice with PBS. The cells were then fixed with aqueous buffered zinc formalin fixative (Z-FIX) for 30 min, permeabilized with 0.1 % Triton X-100 for 5 min, blocked with 1.0 % BSA for 30 min and treated with the mixture of Phalloidin-FITC (0.5 μg/mL) and Hoechst (5 μg/mL) for 30 min at room temperature. After that, the LSCM images of the samples were observed on a LSCM imaging system (Zeiss LSM 780).

Cellular uptake of the nanoparticles measured by flow cytometry. The nanoparticle internalization in U-87 MG, or MCF-7 cells was measured using a flow cytometer (BD LSRFortessa™,

America). 2.0 mL of U-87 MG, or MCF-7 cells in growth medium were seeded into each well of a 6-well culture plate with a cell density of 2.0×10^5 cells/mL and allowed to adhere at 37 °C for 24 h. The growth medium was then replaced with fresh one (2.0 mL, without FBS) containing R6G@FeGd-HN@Pt2 or R6G@FeGd-HN@Pt2@LF/RGD2 ($C_{Fe} = 10 \mu\text{M}$). After further 2 h incubation, the cells were washed twice with PBS, treated with trypsin for 3.0 min and then centrifuged at $500 \times g$ for 5 min. The obtained cells were resuspended in 0.5 mL of PBS and then measured by the flow cytometer. Data analysis was performed using the flow cytometry analysis software (FlowJo7.6).

Cellular uptake of the nanoparticles measured by ICP. 2.0 mL of U-87 MG cells in complete growth medium were seeded into each well of a 6-well culture plate with a cell density of 1.0×10^5 cells/mL and allowed to adhere at 37 °C for 24 h. The growth medium was then replaced with fresh one (2.0 mL, without FBS) without or with FeGd-HN@Pt2@LF/RGD2, or FeGd-HN@Pt2 ($C_{Gd} = 80 \mu\text{M}$). After further 2.0 h incubation, the cells were washed twice with PBS, treated with trypsin for 3.0 min, and then centrifuged at $500 \times g$ for 5 min to remove the extracellular nanoparticles. The obtained cells were used for Gd measurement by ICP.

***In vitro* MRI studies.** The MR imaging and relaxation times of the nanoparticles were tested by a Bruker MRI scanner (7.0 T, B-C 70/16, Bruker, US), or a clinical MRI scanner system (1.5 T, Magnetom Avanto, Siemens, Germany), respectively.

Our FeGd-HN@Pt2@LF/RGD2 nanoparticles were also used as contrast agents for MR imaging of cancer cells compared with FeGd-HN and Magnevist. Typically, 2.0 mL of U-87 MG cells in complete growth medium were seeded into each well of a 6-well culture plate with a cell density of 1.0×10^5 cells/mL and allowed to adhere at 37 °C for 24 h. The growth medium was then replaced with fresh one (2.0 mL, without FBS) without or with FeGd-HN@Pt2@LF/RGD2, or Magnevist[®] ($C_{Gd} = 80 \mu\text{M}$). After further 2.0 h incubation, the cells were washed twice with PBS, treated with trypsin for 3.0 min,

and then centrifuged at $500 \times g$ for 5 min to remove the extracellular nanoparticles. The obtained cells were used for MRI scanning by a Bruker MRI scanner (7.0 T, TE = 10 ms, TR = 250 ms).

Evaluation of intracellular ROS generation via DCF-DA assay. The intracellular generation of ROS was determined by a fluorogenic reagent 2,7-dichlorofluorescein diacetate (DCF-DA), which could be oxidized to the highly fluorescent dichlorofluorescein (DCF) by ROS.

By LSCM. 0.5 mL of U-87 MG cells in complete growth medium were seeded into each well of Falcon® Culture Slide (8 Well, Corning) at a density of 1.0×10^5 cells/mL and allowed to adhere at 37 °C for 24 h. As a control, the cells were pretreated with iron chelator DFO (0.1 mM) or ROS scavenger NAC (5.0 mM) for 1 h to block the ROS generation via Fenton reaction or clean away the intercellular ROS. After that, the growth medium was replaced with a fresh one (without FBS) containing FeGd-HN@Pt2@LF/RGD2, FeCl₃/FeSO₄ (molar ratio 2:1), CDDP, or FeCl₃/FeSO₄ plus CDDP at an equal Fe concentration of 125 μM or Pt concentration of 15.2 μM. After 3.0 h of incubation at 37 °C, the culture media were removed and the cells were washed three times with PBS. After that, 0.5 mL of fresh culture media (with 2 % FBS) containing 20 μM of DCF-DA were added to each well, and the cells were cultured at 37 °C for 30 min. The cells were washed three times with PBS, and then fixed with Z-FIX for 30 min. After that, the LSCM images of the samples were observed on a LSCM imaging system (Zeiss LSM 780).

By flow cytometry analysis. 2.0 mL of U-87 MG in complete growth medium were seeded into each well of a 6-well culture plate with a cell density of 2.0×10^5 cells/mL and allowed to adhere at 37 °C for 24 h. As a control, the cells were pretreated with iron chelator DFO (0.1 mM) or ROS scavenger NAC (5.0 mM) for 1 h to block the ROS generation via Fenton reaction or clean away the intercellular ROS. After that, the growth medium was replaced with a fresh one (without FBS) containing FeGd-HN@Pt2@LF/RGD2 ($C_{Fe} = 125 \mu\text{M}$, $C_{Pt} = 15.2 \mu\text{M}$). After 3.0 h of incubation at 37 °C, the culture media were removed and the cells were washed three times with PBS. After that, 2.0 mL of

fresh culture media (with 2 % FBS) containing 20 μM of DCF-DA were added to each well, and the cells were cultured at 37 °C for 30 min. The cells were washed three times with PBS, treated with trypsin for 3.0 min and then centrifuged at 500 \times g for 5 min. The obtained cells were resuspended in 0.5 mL of PBS and then measured by the flow cytometer (BD LSRFortessaTM, America). Data analysis was performed using the flow cytometry analysis software (FlowJo7.6).

Ferroptosis therapy of cancer cells induced by FeGd-HN@Pt2@LF/RGD2. The ferroptosis therapy efficiency of the nanoparticles was assessed with U-87 MG, or MCF-7 cells by using the MTT method. Typically, 150 μL of U-87 MG or cisplatin-resistant MCF-7 cells in complete DMEM medium were seeded into each well of a 96-well plate at a concentration of 5×10^4 cells/mL and allowed to adhere overnight. The growth medium was replaced with a fresh one (without FBS) containing various concentrations of FeGd-HN@Pt2@LF/RGD2. FeGd-HN, Magnevist, CDDP, and FeCl₃/FeSO₄ (molar ratio 2:1) were used as controls. After 3.0 h of incubation at 37 °C, the growth medium was replaced with complete medium. After further incubation of 45 h, 50 μL of MTT (1.0 mg/mL in PBS) was added to each well of the 96-well plate. After an additional 4.0 h of incubation, the growth medium was removed and the resulted formazan crystals in each well were dissolved with 100 μL of dimethyl sulfoxide (DMSO). The absorbance was recorded at a wavelength of 490 nm using a multi-mode microplate reader (Synergy 2, BioTek Instruments, USA).

To provide further evidence for the ferroptosis therapy of cancer cells induced by our FeGd-HN@Pt2@LF/RGD2 nanoparticles, blocking studies were carried out using iron chelator and ROS scavenger. Before treating with FeGd-HN@Pt2@LF/RGD2 nanoparticles, the cells were pretreated with iron chelator DFO (0.1 mM) or ROS scavenger NAC (5.0 mM) for 1 h to block the ROS generation via Fenton reaction or clean away the intercellular ROS. Other steps were same with the above-mentioned ones.

***In vitro* BBB model studies.** The *in vitro* BBB model was constructed to study the BBB permeability of nanoparticles^{1,2}. Typically, HBEC-5i cells at a density of 1.0×10^5 cells/well were seeded in a 12-well Transwell plate with 0.4 μm of mean pore size membrane, 12 mm diameter of culture plate insert, and 1.1 cm^2 of membrane area (Corning[®] Transwell[®] polyester membrane cell culture inserts). The cell monolayer integrity was monitored everyday using an epithelial volt-ohm meter (Millicell ERS-2, Millipore, USA). The cells with Transendothelial Electrical Resistance (TEER) values above 200 $\Omega\cdot\text{cm}^2$ were chose as the *in vitro* BBB model studies to study the BBB permeability of nanoparticles. The growth medium in the apical chamber (blood side *in vivo*) of the BBB model was replaced with a fresh one containing FeGd-HN@Pt2@LF/RGD2, or FeGd-HN ($C_{Gd} = 60 \mu\text{M}$, 0.7 mL), and then cultured for 12 h at 37 °C. During the incubation, the TEER values were measured to be over 200 $\Omega\cdot\text{cm}^2$. After that, the culture media in the apical chamber and basolateral chamber were collected to measure the C_{Gd} by ICP-OES.

To provide further evidence for the LF-mediated transcytosis mechanism, a blocking study was also carried out by incubating FeGd-HN@Pt2@LF/RGD2 ($C_{Gd} = 60 \mu\text{M}$) in the apical chamber in the presence of 15 times of LF.

MRI of mouse brain for *in vivo* BBB studies. All animal experiments were approved by the Animal Care and Use Committee of the National Institutes of Health Clinical Center (ACUC/ NIH CC). The normal nude mice without tumors were anaesthetized by isoflurane (1.0-2.0%) in oxygen, and placed in an animal-specific brain coil for MRI data acquisition. Mice were kept warm by circulating warm water (37 °C), and were placed in a stretched prone position with a respiratory sensor during the experiments. T_1 -weighted images were acquired at pre-injection and post injection (intravenously). Multi-slice multi-echo sequence was employed to acquire images using parameters as follows: repetition time (TR) = 800 ms, echo time (TE) = 8 ms, flip angle = 180°, matrix size = 256 × 256, field of view = 30 × 30 mm^2 , slices = 16, slice thickness = 1.2 mm. MR images were analyzed by

measuring signal intensity with the software Image J. The signal-to-noise ratio (SNR) and SNR ratio (*i.e.* signal enhancement) were calculated according to the equation (1) and (2).

$$\text{SNR} = \text{SI}_{\text{mean}} / \text{SD}_{\text{noise}} \quad (1)$$

$$\Delta\text{SNR} = (\text{SNR}_{\text{post}} - \text{SNR}_{\text{pre}}) / \text{SNR}_{\text{pre}} \times 100 \% \quad (2)$$

***T*₁-weighted MRI of subcutaneous tumors.** The U-87 MG tumor-bearing nude mice were prepared by inoculating U-87 MG cells (4×10^6 cells in 100 μL PBS) into the right leg of each mouse (female, 5 weeks) under anesthesia. The tumor size was measured *via* a caliper at predetermined times. The tumor volume was calculated through $ab^2/2$, where *a* and *b* are respectively the length and width of a tumor.

The U-87 MG tumor-bearing nude mice were anaesthetized by isoflurane (1.0-2.0%) in oxygen, and placed in an animal-specific body coil for MRI data acquisition. Mice were kept warm by circulating warm water (37 °C), and were placed in a stretched prone position with a respiratory sensor during the experiments. *T*₁-weighted images were acquired at pre-injection and post injection (intravenously) of FeGd-HN@Pt₂, or FeGd-HN@Pt₂@LF/RGD₂ ($C_{\text{Gd}} = 5.0 \text{ mg / kg}$). Multi-slice multi-echo sequence was employed to acquire images using parameters as follows: repetition time (TR) = 400 ms, echo time (TE) = 8 ms, flip angle = 180°, matrix size = 256 \times 256, field of view = 40 \times 40 mm², slices = 16, slice thickness = 1 mm. MR images were analyzed by measuring signal intensity with the software Image J. The Signal-to-Noise Ratio (SNR) and ΔSNR (*i.e.* signal enhancement) were calculated according to the equation (1) and (2).

Studies on the orthotopic brain tumor-bearing mice

Orthotopic brain tumor growth and survival of the mice. Six-week-old female BALB/C nude mice were orthotopically implanted with U87/GFP/Luc cells (1×10^6 cells/mouse). Tumor-bearing mice were monitored using *in vivo* luciferase imaging. Mice were sedated with Isoflurane through a nose cone and subsequently received an intraperitoneal injection of the substrate D-luciferin (1.5 mg/mouse; Caliper Life Sciences). After 5 min of luciferin administration, images were acquired using

IVISTM 100 (Xenogen Corp.). Signal intensity was quantified using the Living image software version 2.6.1 (Xenogen Corp.). At 7 days after implantation, the mice were treated with FeGd-HN@Pt2@LF/RGD2 nanoparticles, FeGd-HN@Pt2@RGD2 nanoparticles, FeGd-HN@Pt2 nanoparticles, FeGd-HN nanoparticles ($C_{Fe} = 3.6$ mg / kg, $C_{Gd} = 5.0$ mg / kg, $C_{Pt} = 1.5$ mg / kg), or Saline every 3 days for 9 days. Five mice were used for each group. The percent survival of mice in each group was measured until all the mice used had been sacrificed.

MRI of the orthotopic brain tumors. Diffusion weighted MRI (DW-MRI or DWI) were performed on a Bruker Biospin 9.4T animal MRI scanner (Bruker, Germany) equipped with a horizontal bore (diameter, 30 cm; gradient strength, 734 mT/m). The gradients were applied in three orthogonal directions.

Immunohistochemistry staining of the orthotopic brain tumors. Immunohistochemistry staining was conducted according to standard procedures. Sections were deparaffinized, washed, and preincubated in a blocking solution (1% bovine serum albumin in 0.05 M Tris-buffered saline), followed by incubation with primary antibodies (anti-Ki-67 antibody, Abcam) and species-matched secondary antibodies (ChemMate EnVision™; Dako A/S, Glostrup, Denmark), after which the sections were again washed, visualized with diaminobenzidine (DAB), and nuclear counterstained with hematoxylin. Images were analyzed with ImageJ 7.0 software.

Statistical analysis. Statistical significance was determined by applying Student's *t*-test or by a one-way ANOVA followed by Student-Newman-Keuls test using Sigma Stat version 3.5. The significance level was fixed as $P < 0.05$.

References

- [1] Ni, D.; Zhang, J.; Bu, W.; Xing, H.; Han, F.; Xiao, Q.; Yao, Z.; Chen, F.; He, Q.; Liu, J.; Zhang, S.; Fan, W.; Zhou, L.; Peng, W.; Shi, J. Dual-Targeting Upconversion Nanoprobes across the Blood–Brain Barrier for Magnetic Resonance/Fluorescence Imaging of Intracranial Glioblastoma. *ACS Nano* **2014**, *8*, 1231-1242.
- [2] Qiao, R.; Jia, Q.; Huwel, S.; Xia, R.; Liu, T.; Gao, F.; Galla, H. J.; Gao, M. Receptor-Mediated Delivery of Magnetic Nanoparticles across the Blood-Brain Barrier. *ACS Nano* **2012**, *6*, 3304-3310.

Table S1. Synthesis conditions and characterization results of the FeGd-HN@Pt nanoparticles

Sample Nomenclature	CDDP ^a (mL)	Pt Loading Content (%) ^b	Pt Loading Efficiency (%) ^c	H ₀ (T) ^d	r_1 (mM ⁻¹ s ⁻¹) (Gd) ^e	r_2 (mM ⁻¹ s ⁻¹) (Fe) ^e	r_2 / r_1 ^e
FeGd-HN@Pt1	0.2	5.3±0.3	52.6±1.8	7.0	17.51	45.70	2.61
FeGd-HN@Pt2	0.4	6.9±0.4	39.7±1.1	7.0	15.83	52.32	3.30
FeGd-HN@Pt3	0.8	8.9±0.4	24.9±1.3	7.0	13.21	63.14	4.78
FeGd-HN@Pt4	1.5	11.9±0.6	15.6±0.6	7.0	N/A	N/A	N/A
FeGd-HN@Pt5	3.0	11.4±0.7	7.5±0.4	7.0	N/A	N/A	N/A

^a The feeding amount of CDDP (4.0 mg/mL in DMF) mixed with FeGd-HN solutions (5.0 mL, C_{Fe} =5.50 mM, C_{Gd} =2.69 mM).

^b Calculated from the mass percentage of the loaded Pt to the nanoparticle FeGd-HN@Pt (mean ± SD, $n = 3$).

^c Calculated from the mass percentage of the loaded Pt to the feeding Pt (mean ± SD, $n = 3$).

^d The r_1 and r_2 are measured on a MRI scanner system (7.0 T, Bruker, B-C 70/16 US).

^e Calculated according to the Gd or Fe concentrations.

Table S2. r_1 and r_2 values under different magnetic fields

Sample Nomenclature	H_0 (T) ^a	r_1 (mM ⁻¹ s ⁻¹) (Gd) ^b	r_2 (mM ⁻¹ s ⁻¹) (Fe) ^b	r_2 / r_1
FeGd-HN@Pt2	7.0	15.83	52.32	3.30
	1.5	67.75	72.01	1.06
FeGd-HN@Pt2@LF/RGD2	7.0	12.70	50.72	3.99
	1.5	56.57	70.56	1.25

^a The r_1 and r_2 are measured on a MRI scanner system (7.0 T, Bruker, B-C 70/16 US), and a clinical MRI scanner system (1.5 T, Magnetom Avanto, Siemens, Germany)

^b Calculated according to the Gd or Fe concentrations.

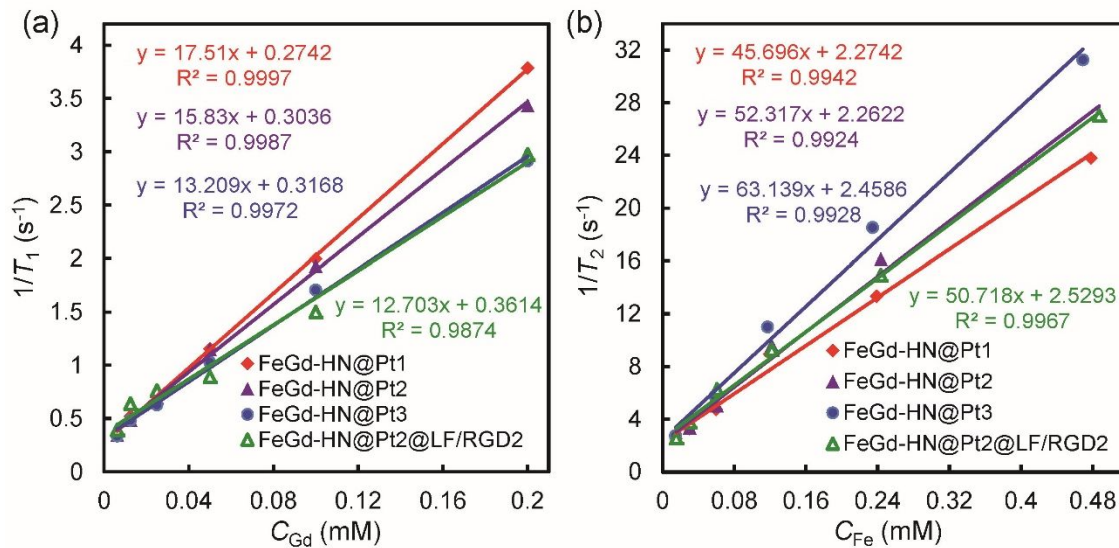


Figure S1. (a): T_1 relaxation rate plotted as a function of C_{Gd} for FeGd-HN@Pt1-3, or FeGd-HN@Pt2@LF/RGD2. (b): T_2 relaxation rate plotted as a function of C_{Fe} for FeGd-HN@Pt1-3, or FeGd-HN@Pt2@LF/RGD2. Magnetic field: 7.0 T. For T_1 relaxation rates: TE = 10 ms, TR = 100 ~ 4000 ms. For T_2 relaxation rates: TR = 2000 ms, TE = 10 ~160 ms.

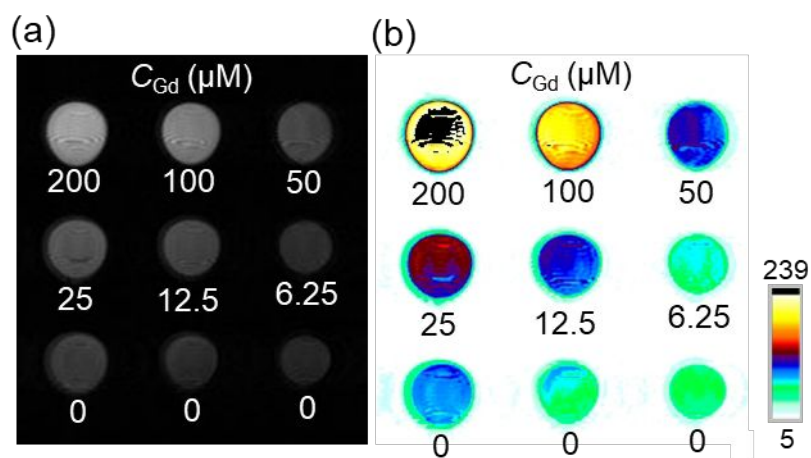


Figure S2. (a): T_1 -weighted MR images of FeGd-HN@Pt2@LF/RGD2 with various C_{Gd} (6.25 ~ 200 μM) (TE = 10 ms, TR = 500 ms). Magnetic field = 7.0 T. (b): The corresponding color images.

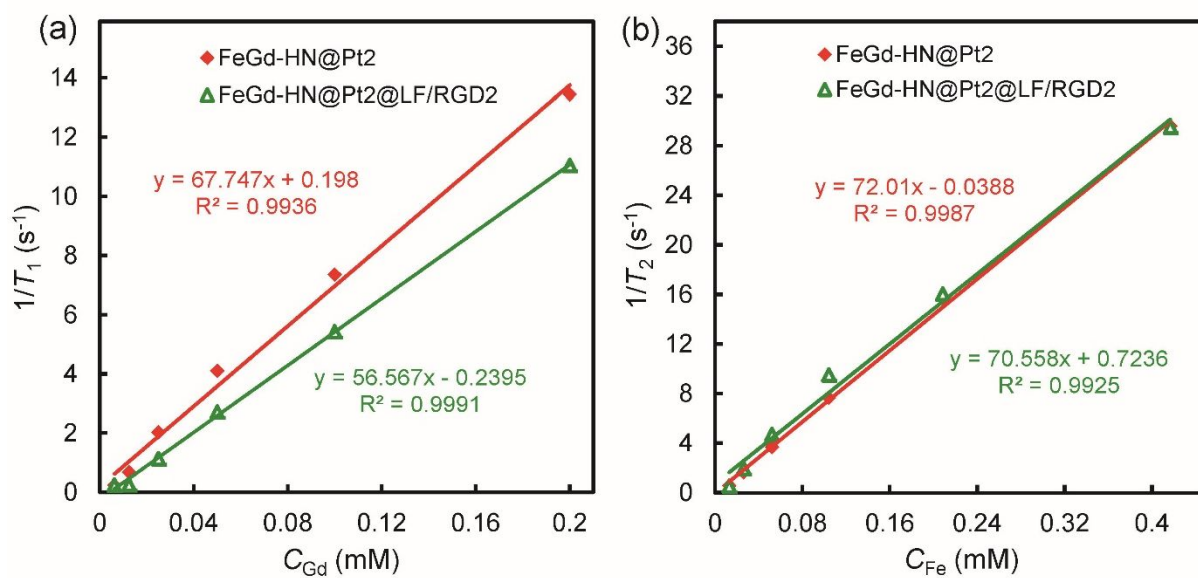


Figure S3. (a): T_1 relaxation rate plotted as a function of C_{Gd} for FeGd-HN3@Pt2, or FeGd-HN3@Pt2@LF/RGD2. (b): T_2 relaxation rate plotted as a function of C_{Fe} for FeGd-HN3@Pt2, or FeGd-HN3@Pt2@LF/RGD2. Magnetic field: 1.5 T.

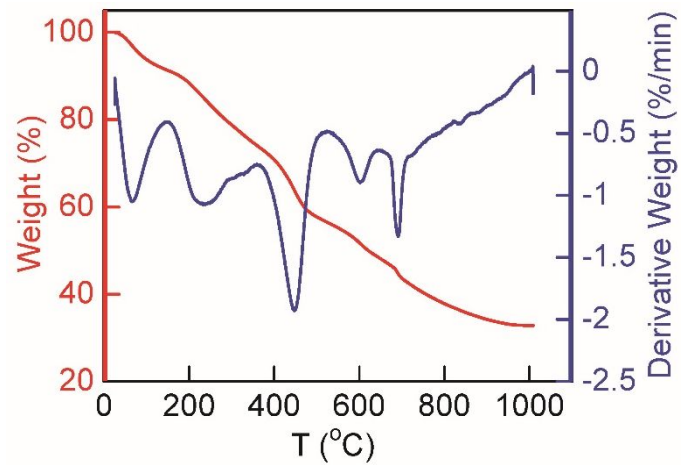


Figure S4. Thermogravimetry (TGA) and differential thermogravimetry (DTG) curves of FeGd-HN@Pt2@LF/RGD2.

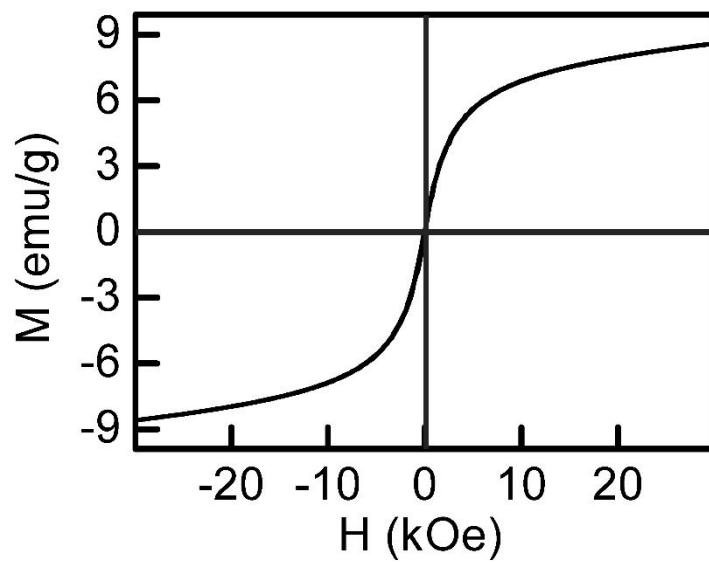


Figure S5. Field-dependent magnetization curve ($H - M$) of FeGd-HN@Pt2@LF/RGD2 at 300 K. The saturation magnetization (M_s) value was determined to be 8.6 emu/g.

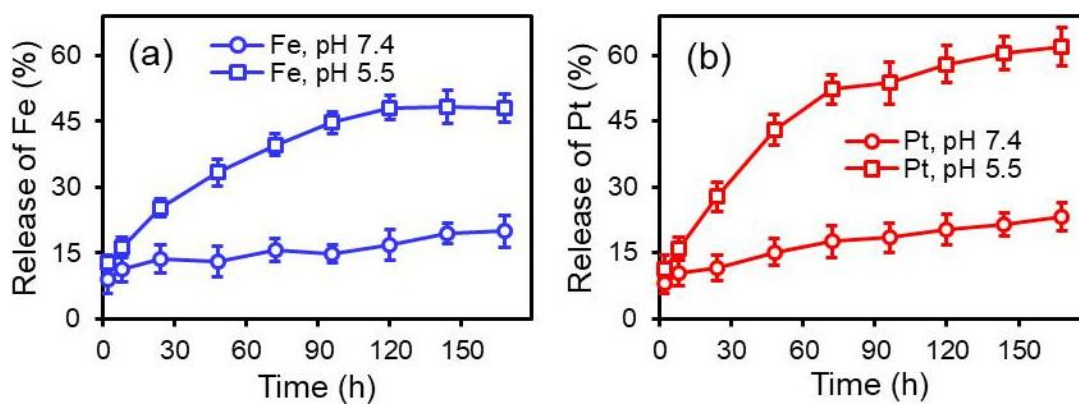


Figure S6. Release behaviors of Fe (a) or Pt (b) from FeGd-HN@Pt₂@LF/RGD2 at 37 °C in PBS with different pH values.

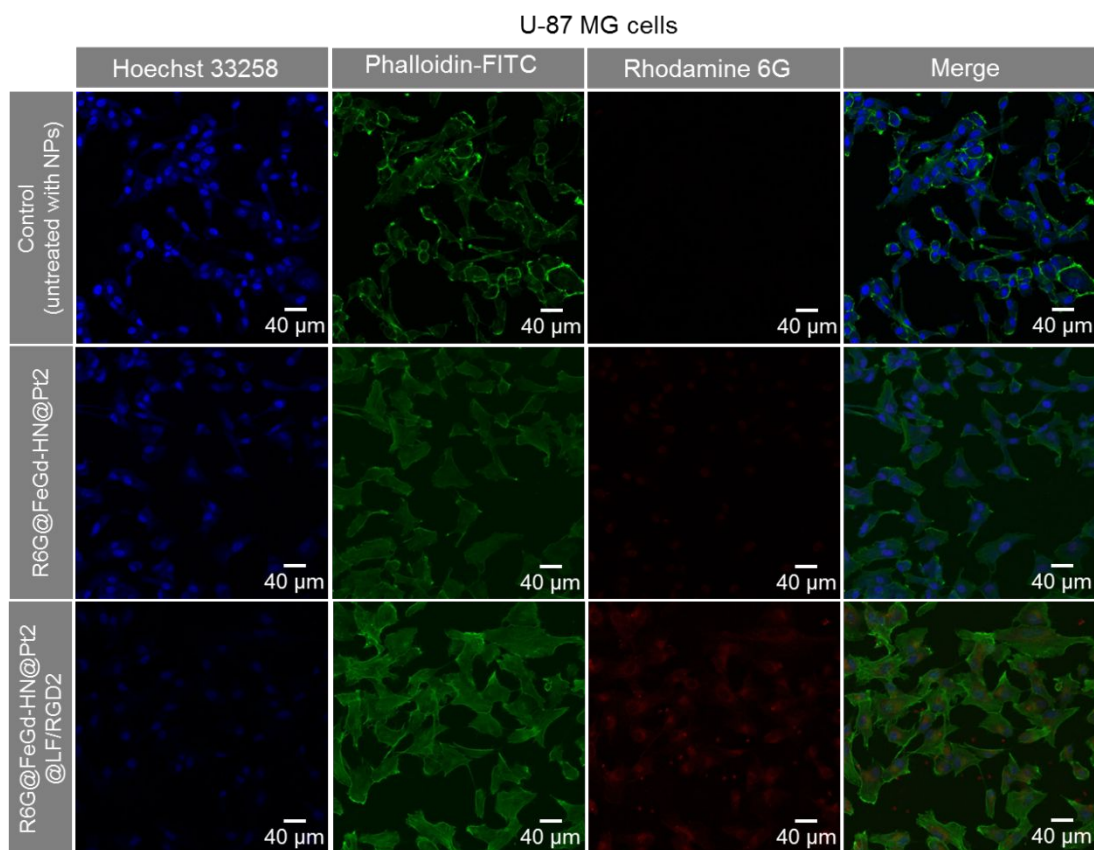


Figure S7. LSCM images of U-87 MG cells incubated with R6G@FeGd-HN@Pt2 or R6G@FeGd-HN@Pt2@LF/RGD2. The cells untreated with nanoparticles are used as the control. The nucleus stained with Hoechst 33258 is blue, and the cytoskeleton stained with phalloidin-FITC is green. The R6G-loaded nanoparticles are red.

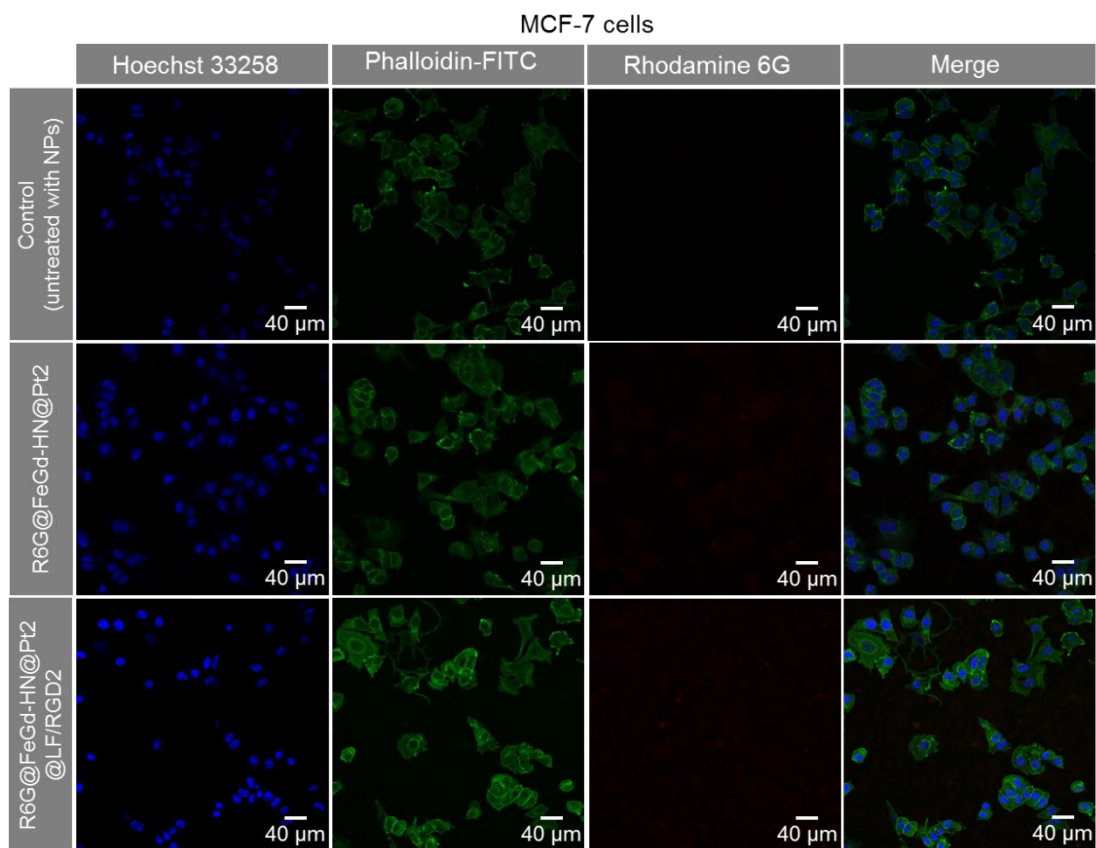


Figure S8. LSCM images of MCF-7 cells incubated with R6G@FeGd-HN@Pt2 or R6G@FeGd-HN@Pt2@LF/RGD2. The cells untreated with nanoparticles are used as the control. The nucleus stained with Hoechst 33258 is blue, and the cytoskeleton stained with phalloidin-FITC is green. The R6G-loaded nanoparticles are red.

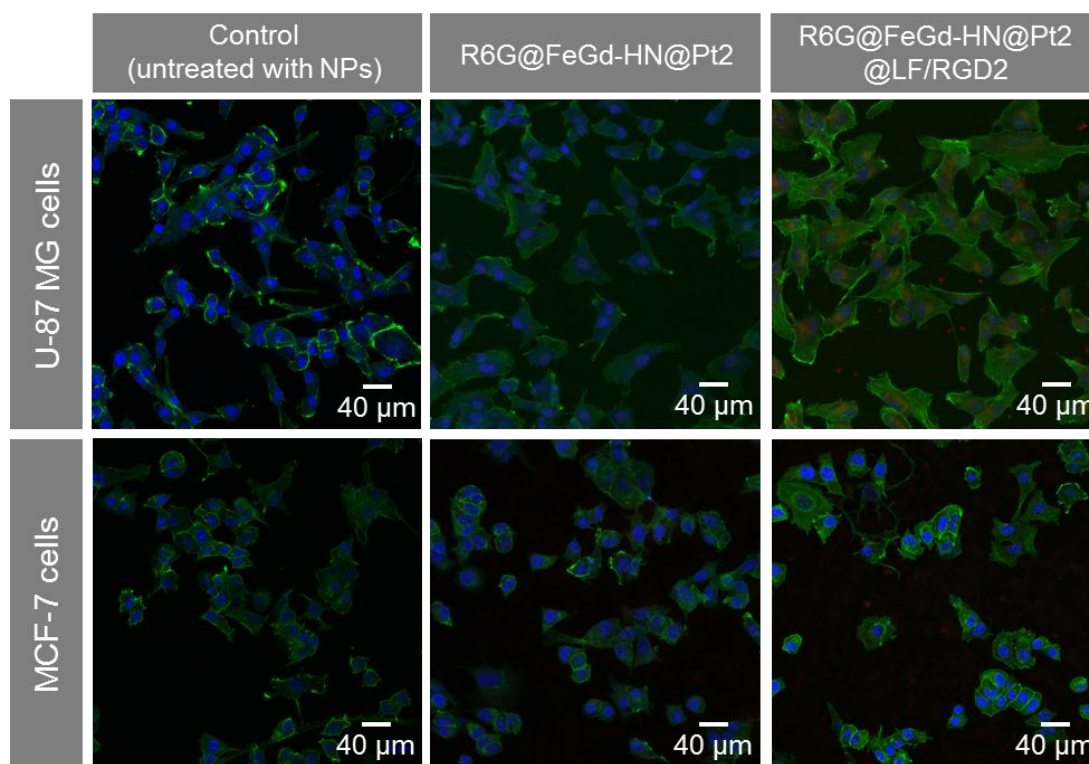


Figure S9. LSCM images of U-87 MG or MCF-7 cells incubated with R6G@FeGd-HN@Pt2 or R6G@FeGd-HN@Pt2@LF/RGD2. The cells untreated with nanoparticles are used as the control. The cytoskeleton stained with phalloidin-FITC is green and the nucleus stained with Hoechst is blue. The R6G-loaded nanoparticles are red.

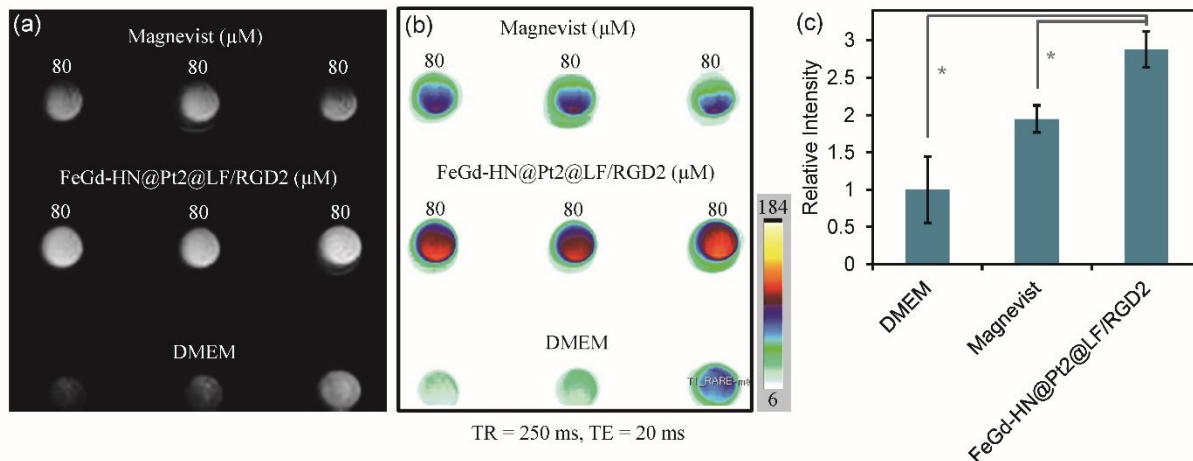


Figure S10. (a): T_1 -weighted MR images of U-87 MG cells with various contrast agents. (b): The corresponding color MR images. (c): Relative intensities of the MR images in (a) compared with the control (DMEM without contrast agents), which is measured by the ImageJ. Magnetic field = 7.0 T. Mean \pm SD, $n = 3$. * $P < 0.01$.

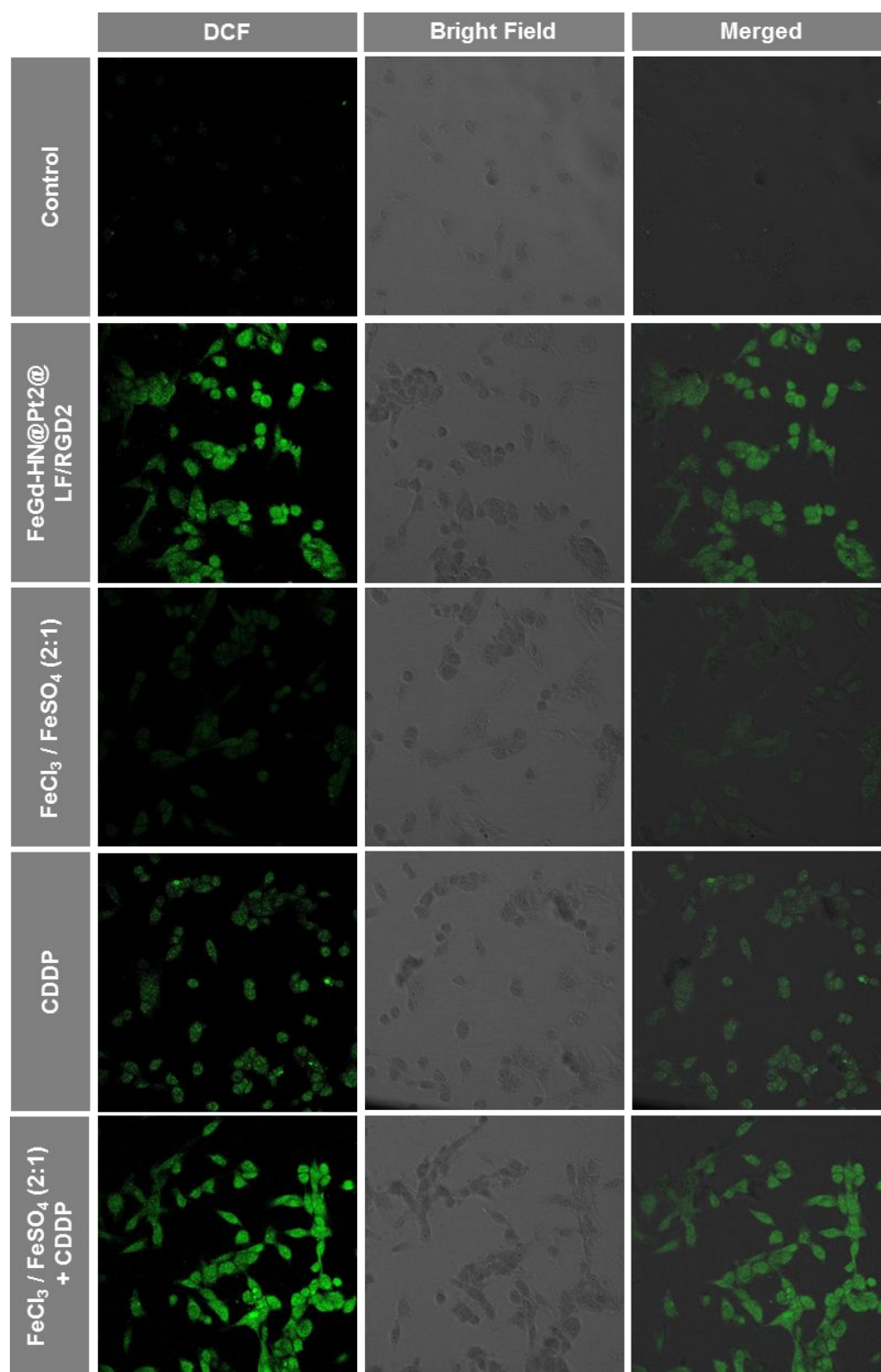


Figure S11. Evaluation of intracellular ROS generation *via* DCF-DA assay observed by LSCM. The U-87 MG cells were incubated with FeGd-HN3@Pt2@LF/RGD2, FeCl₃/FeSO₄ (molar ratio 2:1), CDDP, or FeCl₃/FeSO₄ plus CDDP at an equal Fe concentration of 125 μM or Pt concentration of 15.2

μM . The untreated cells were used as a control. DCF-DA (20 μM) incubated with the cells can be oxidized to highly fluorescent DCF by intracellular ROS.

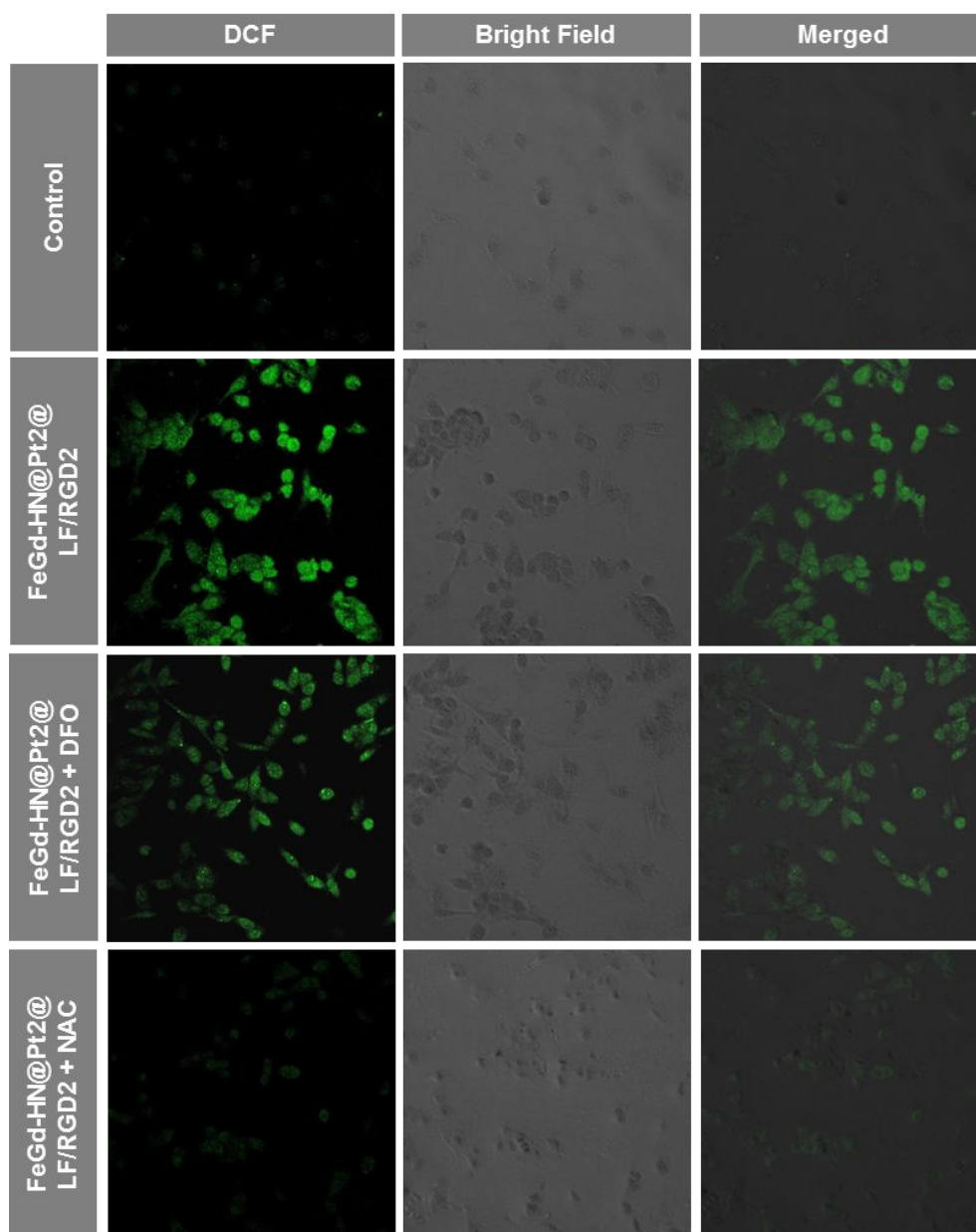


Figure S12. Evaluation of intracellular ROS generation *via* DCF-DA assay observed by LSCM. The U-87 MG cells were incubated with or without FeGd-HN@Pt2@LF/RGD2 ($C_{Fe} = 125 \mu\text{M}$). DCF-DA ($20 \mu\text{M}$) incubated with the cells can be oxidized to highly fluorescent DCF by intracellular ROS. As a control, the cells were pretreated with iron chelator DFO (0.1 mM) or ROS scavenger NAC (5.0 mM) for 1.0 h to block the ROS generation via Fenton reaction or clean away the intercellular ROS.

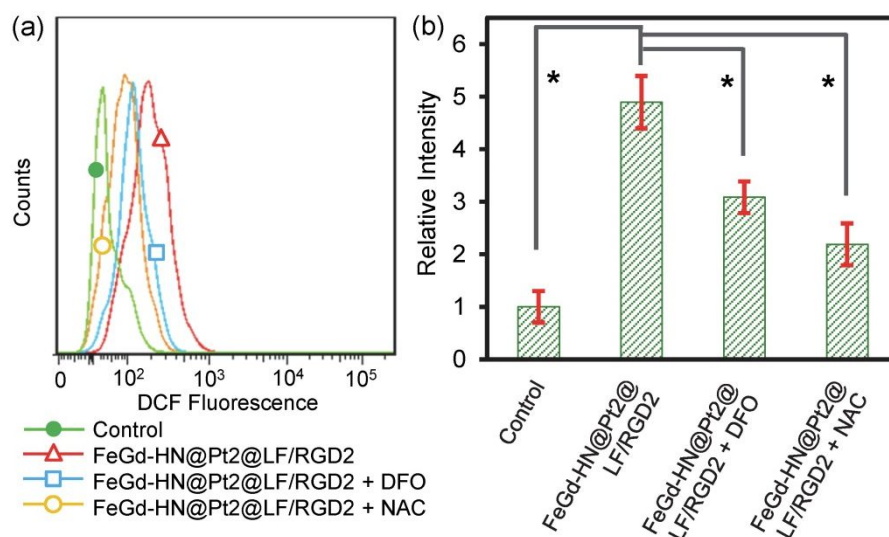


Figure S13. Evaluation of intracellular ROS generation *via* DCF-DA assay measured by flow cytometry. The U-87 MG cells were incubated with or without FeGd-HN@Pt2@LF/RGD2 ($C_{Fe} = 125 \mu\text{M}$). DCF-DA ($20 \mu\text{M}$) incubated with the cells can be oxidized to highly fluorescent DCF by intracellular ROS. As a control, the cells were pretreated with iron chelator DFO (0.1 mM) or ROS scavenger NAC (5.0 mM) for 1.0 h to block the ROS generation via Fenton reaction or clean away the intercellular ROS. (a): The DCF fluorescence distributions of U-87 MG cells with different treatments. (b): The relative intensity (i.e. mean fluorescence intensity ratio) of the treated U-87 MG cells to that of the untreated cells. Mean \pm SD, $n = 3$. * $P < 0.01$.

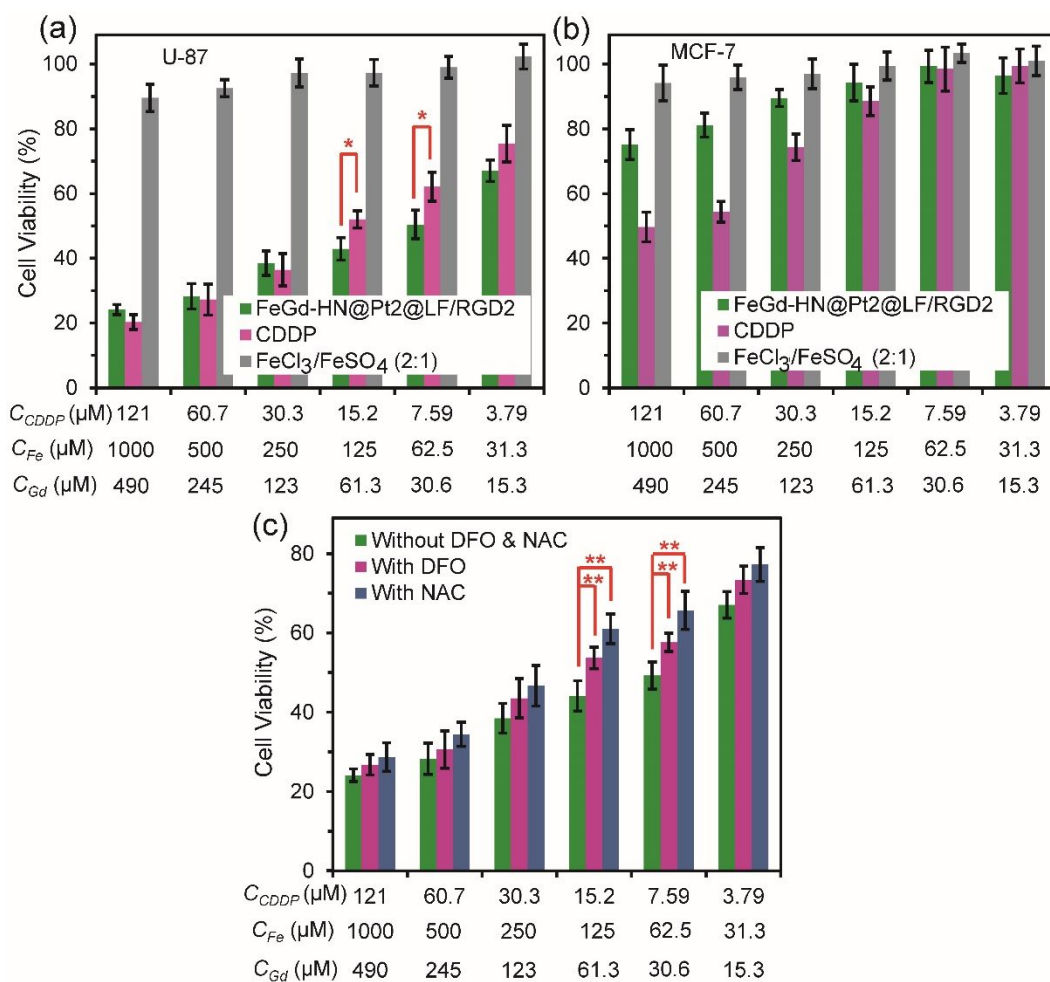


Figure S14. Evaluation of the ferroptosis therapy efficiency. (a, b): Ferroptosis therapy efficiency of FeGd-HN@Pt2@LF/RGD2, CDDP, or FeCl₃/FeSO₄ (molar ratio 2:1) on U-87 MG cells (a) or MCF-7 cells (b). (c): Blocking of the ferroptosis therapy induced by FeGd-HN@Pt2@LF/RGD2. Iron chelator DFO = 0.1 mM. ROS scavenger NAC = 5.0 mM. Mean \pm SD, n = 4. * P < 0.01, ** P < 0.01.

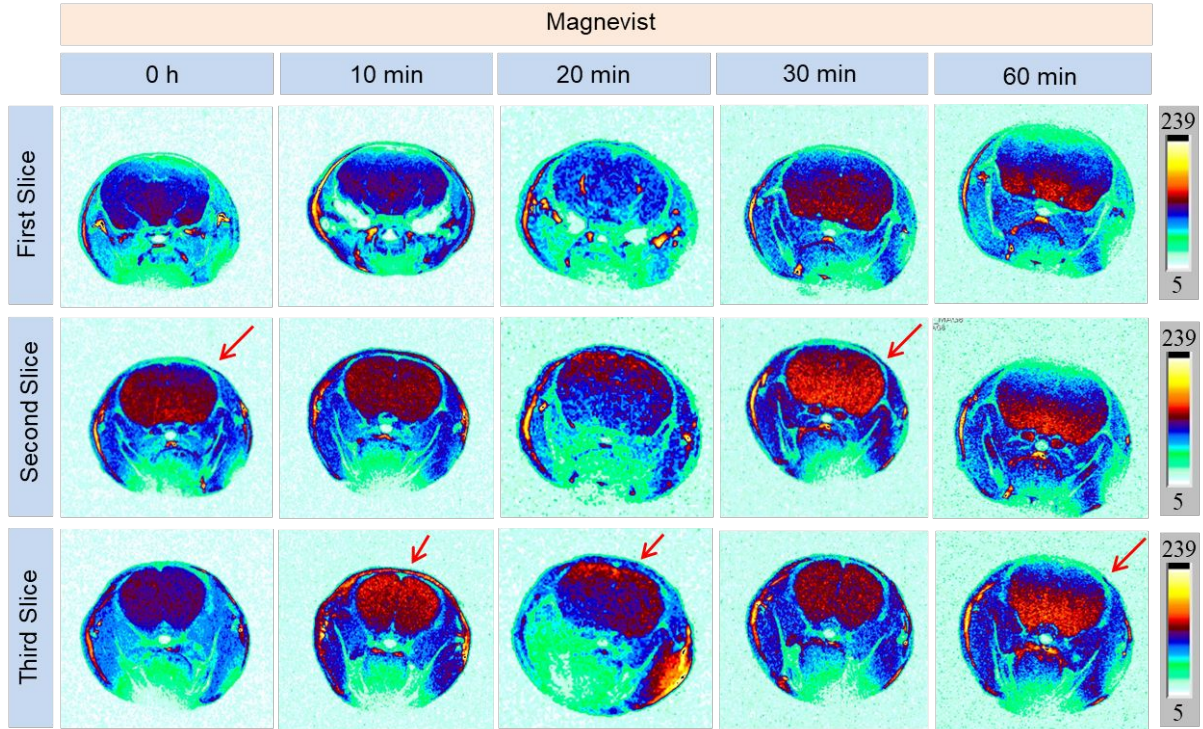


Figure S15. T_1 -weighted MR images of mouse normal brains (without tumors) at different slices before or after intravenous injection of Magnevist ($C_{Gd} = 5.0$ mg / kg).

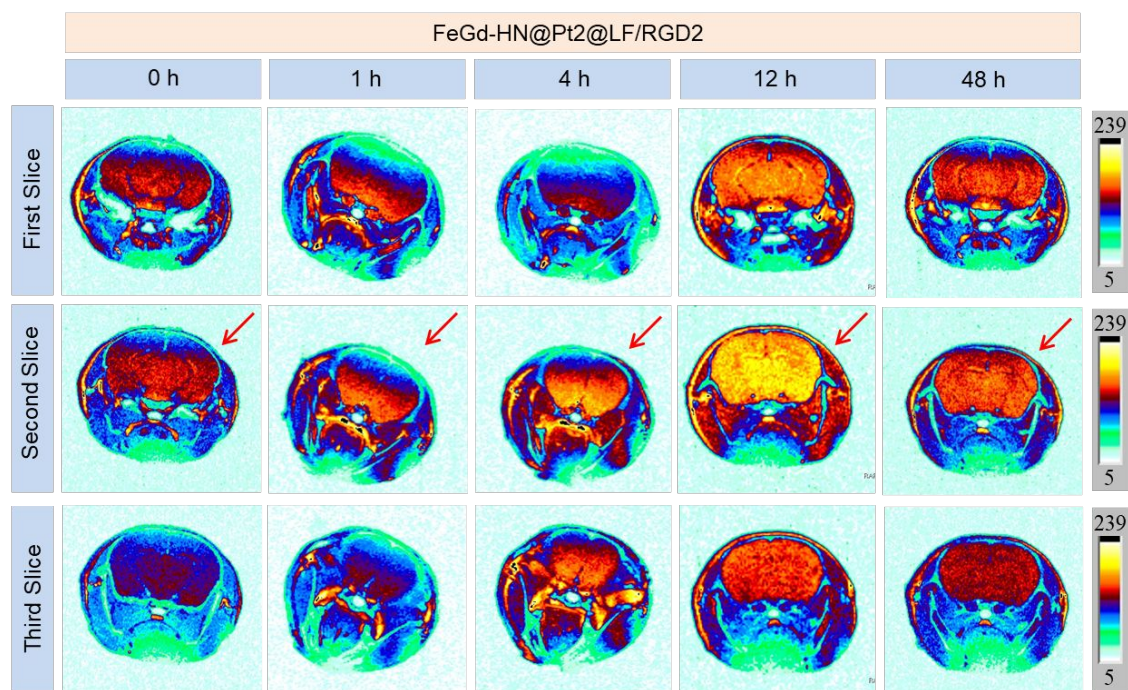


Figure S16. T_1 -weighted MR images of mouse normal brains (without tumors) at different slices before or after intravenous injection of FeGd-HN@Pt2@LF/RGD2 ($C_{Gd} = 5.0$ mg / kg).

FeGd-HN@Pt2@LF/RGD2

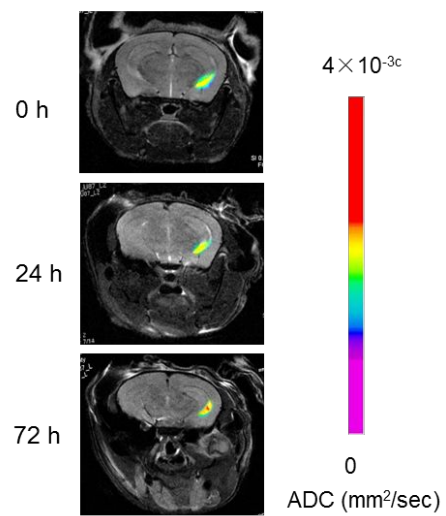


Figure S17. ADC parametric maps of the orthotopic brain tumor-bearing mice before or after treatment with FeGd-HN@Pt2@LF/RGD2.

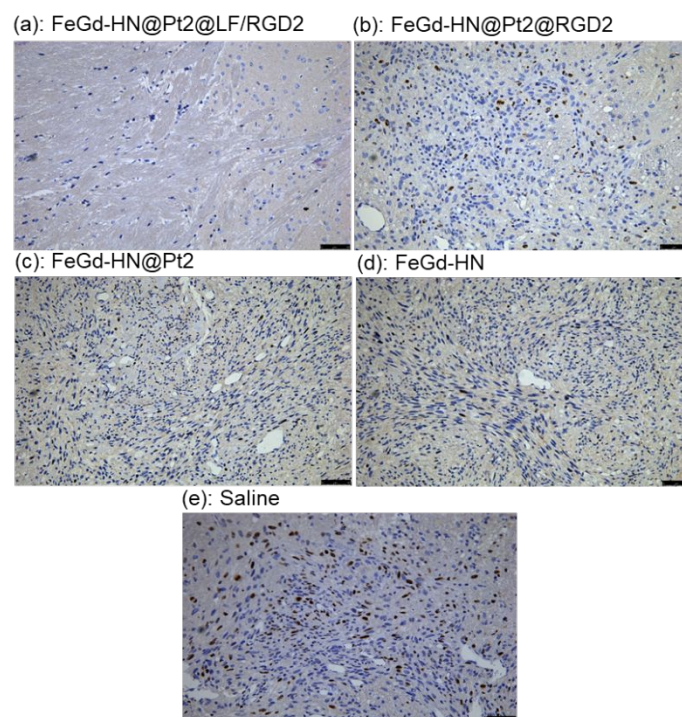


Figure S18. Immunohistochemistry analysis of the orthotopic brain tumors stained with Ki-67 antibody after treatments with FeGd-HN@Pt2@LF/RGD2 (a), FeGd-HN@Pt2@RGD2 (b), FeGd-HN@Pt2 (c), FeGd-HN (d), or Saline (e) at 48 h post injection. Scale bar 100 μ m.

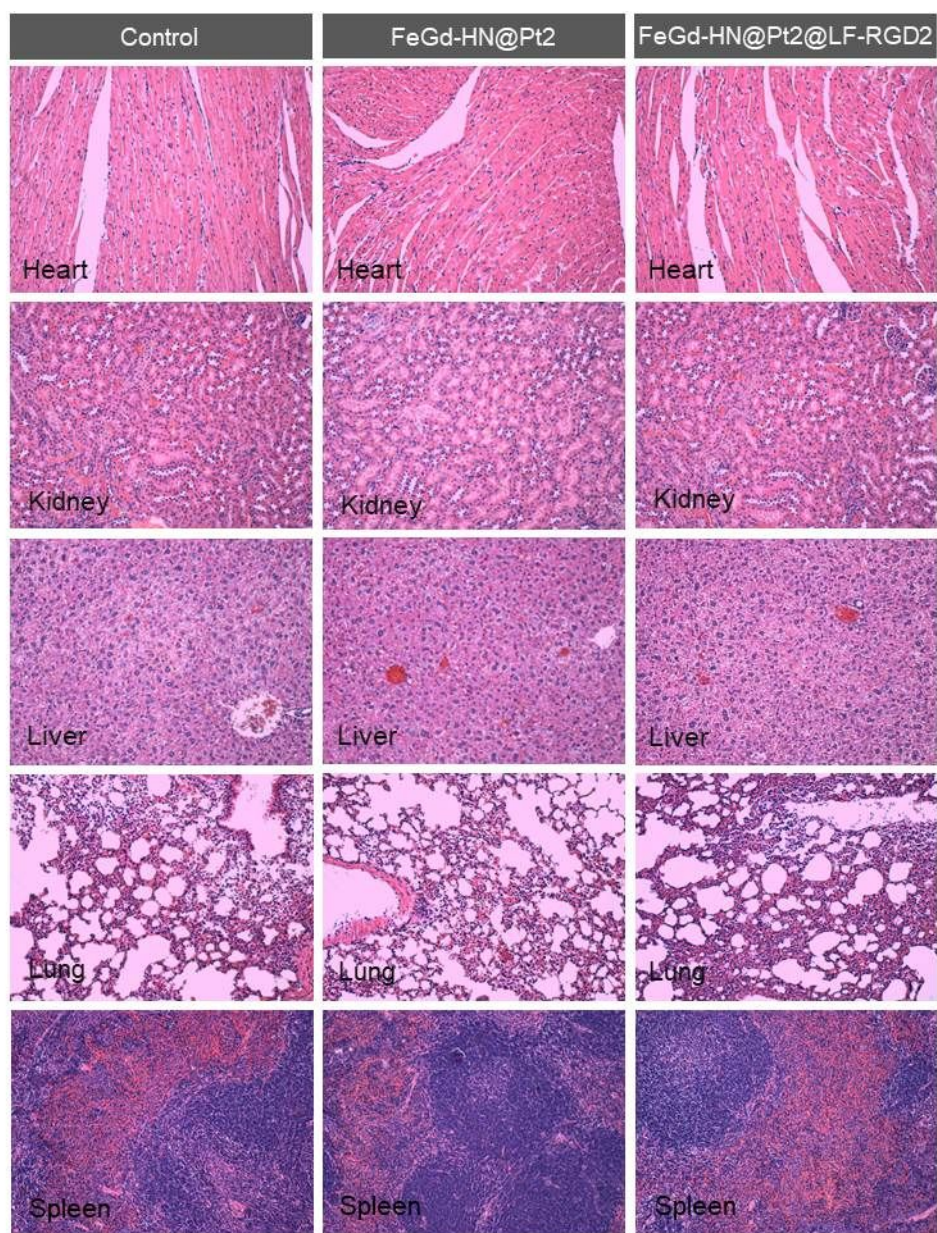


Figure S19. Histological analyses of main organs from the normal mice without tumors (control), and that with intravenous injection of FeGd-HN@Pt₂, or FeGd-HN@Pt₂@LF/RGD₂ nanoparticles (5.0 mg/kg). The organs were collected at 48 h post injection. Comparing with the control, FeGd-HN@Pt₂, and FeGd-HN@Pt₂@LF/RGD₂ did not exhibit obvious toxicity to the major organs, indicating good biocompatibility of our nanoparticles.